Moving Molecules in Crystalline Solids: Gradual Structure Transition and Spin Transition/Crossover

IOP Conf. Series: Materials Science and Engineering **515** (2019) 012001 doi:10.1088/1757-899X/515/1/012001

Moving Molecules in Crystalline Solids: Gradual Structure Transition and Spin Transition/Crossover

Takayuki Ishida

Department of Engineering Science, The University of Electro-Communications, 1-5-1 Chofugaoka, Chofu, Tokyo 182-8585, Japan

Corresponding author's email: takayuki.ishida@uec.ac.jp

Abstract. Magnetic switches working in solid states are of recent interest for applications to sensor, memory, etc. The author and co-workers have developed various unconventional spin transition/crossover materials. The first example is a supramolecular chemistry consisting of genuine organic nitroxide biradicals with a triplet ground state. Each nitroxide group is located close to each other to form weak covalent bonds in an intermolecular fashion. Biradicals are polymerized/depolymerized stepwise. The second example belongs to 3d-2p heterospin systems where the nitroxide oxygen atom is directly bonded to a nickel(II) or copper(II) ion. The planar/nonplanar chelate structure changes, accompanied by high-/low-spin transition due to a 3d-2p exchange-coupling switch. A novel entropy-driven spin crossover scenario has been established. The third example is a 3d iron(II) spin crossover material carrying a stearyl (C_{18}) group. An order-disorder-type structural transition appears with respect to the alkyl conformation. As these examples show, single-crystal-to-single-crystal structural transitions are often observed. It is because the spin entropy term regulates the atomic dislocation enthalpy, and the entropy change due to the spin multiplicity is basically small. These molecular motions clarified by means of detailed crystallography afford one of the most convincing evidence for the spin transition phenomenon.

Keywords: Spin transition, Solid-state chemistry, Exchange coupling, Heterospin, Radical

1. Introduction

Various magnetic switches working in solid states are of recent interest for pursuing applications to smart materials like sensor, memory, display, and so on [1–5]. A reversible spin transition between low-spin (LS) and high-spin (HS) states associated with external stimuli like heat, pressure, and light is called spin crossover (SCO) [1–4]. Iron(II) compounds are the most popular, because drastic magnetic and chromic changes are expected between $S = 0$ and $S = 2$ states from the $3d^6$ electron configuration. Bistability with a thermal hysteresis, hopefully near room temperature, is a key to applications under ambient conditions (Figure 1a). Spin transition behavior has so far been investigated in coordination compounds extensively. Organic paramagnetic species are also available for a spin carrier [6,7]. Furthermore, heterospin systems have an advantage in utilizing various symmetries and energy levels of magnetic orbitals, in the context of frontier-orbital engineering.

There have been a number of organic (2p) spins and related heterospin systems developed [6,7] because of a wide variety of derivatizations owing to sophisticated synthetic techniques. In this report three examples will appear, which show spin transition concomitant with notably gradual crystal structure transition. Paramagnetic materials are given from organic free radicals (genuine 2p spin systems) and coordination compounds involving paramagnetic ligands (3d-2p heterospin systems). The third example belongs to 3d spin iron(II) SCO systems. A main subject of this paper is to introduce them and discuss the magneto-structure correlation on the basis of detailed crystallographic analysis.

Spin transition phenomena are regulated by the compensation of enthalpy loss and entropy gains [3]; LS states are favorable for the enthalpy term in a low-temperature (LT) phase, while HS states for the entropy term in a high-temperature (HT) phase (Figure 1b). Paramagnetic centers move in crystals to satisfy thermodynamic conditions, so that the intermolecular distances or intramolecular bond angles would change. The soft character in organic materials/crystals plays an essential role in accommodation of structural modification. Single-crystal-to-single-crystal structural transformation is very helpful to the detailed studies, and thanks to this we will witness that molecules often move and struggle in crystalline solids.

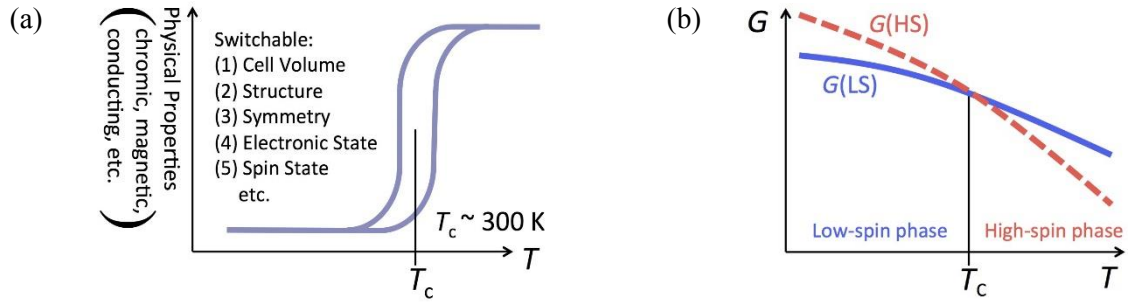

Figure 1. (a) Room-temperature phase transition attracts much attention to materials researchers. (b) Gibbs energy diagram for LS/HS transition materials.

2. Spin transition materials from 2p systems

The nitroxide (aminoxyl) chromophore is ideal for the study of magnetic exchange interactions because of the persistency as an isolable paramagnetic species. Actually the low-lying ferromagnetic state has been well established with pioneering works on *m*-phenylene-bridged bis-, tris-, and oligo-nitroxides [7–10]. Organic HS molecules are realized under certain conditions when nonbonding molecular orbitals are available. There have been many reports on the theory and experiments about biradicals and dicarbenes [7]. The mechanism on π-topological degeneracy has been explained in terms of the Kekulé/non-Kekulé classification, spin-polarization scheme, star/non-star rule, or disjoint/non-disjoint MO theorem [7,11,12]. These logics have originally been proposed for hydrocarbon systems like *p*- and *m*-quinodimethanes, but they also hold for systems involving nitroxide spin centers [10], as illustrated with Scheme 1. A simple and typical explanation for *p*- and *m*-phenylene bis(nitroxides) is as follows: A Kekulé structure can be drawn for the former (Scheme 1a), leading to a diamagnetic character. In contrast, a biradical character remains in any canonical structural formulas for the *m*-phenylene isomer (Scheme 1b). Hund's rule is operative in the latter, affording a biradical nature with the triplet state stabilized. In fact, strong intramolecular ferromagnetic coupling gave a wide energy-gap of singlet and triplet states typically for *m*-phenylene bis(nitroxides) [13] and heteroaromatic 1,3-diyl bis(nitroxides) [14–16]. Characteristic decomposition reactions have also been reported owing to the considerable spin density delocalized on the adjacent aromatic ring [17–19].

Scheme 1. Canonical structures of (a) *p*- and (b) *m*-phenylene-bridged bisnitroxides.

Based on the successful results on such prototypes, author's group moved on to supramolecular chemistry with the ground HS molecules as a starting material. In the present study, several derivatives of BPBN (biphenyl-3,5-diyl bis(*tert*-butyl nitroxide); Scheme 2) were synthesized [20–24]. Methyl groups and fluorine atoms were substituted at the 2,5-positions on the outer phenyl ring. The Suzuki cross-coupling reaction [25] is a key step, where a variety of commercially available aryl boronic acids are coupled with an important synthetic intermediate, 1-bromo-3,5-bis(*N*-*tert*-butylhydroxylamino)benzene. It is very helpful for synthetic chemists that unprotected hydroxylamino groups did not poison the Suzuki coupling catalyst.

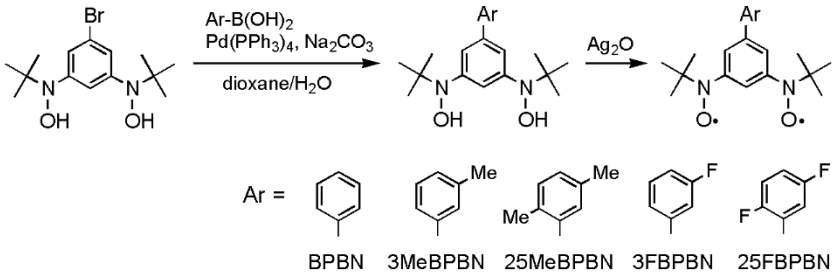

Scheme 2. Synthesis of BPBN derivatives.

The magnetic susceptibilities of polycrystalline BPBN derivatives were measured on a SQUID susceptometer in a typical temperature scan range 1.8 – 360 K (Figure 2). The $\chi_m T(T)$ profiles of β-BPBN [21] and β-25MeBPBN [22] showed 0.95 cm^3 K mol^{-1} as the HT limit, being close to the theoretical triplet value of 1.00 cm^3 K mol^{-1}. Compounds BPBN and 25MeBPBN can afford room-temperature triplet molecular solids. This finding implies that the intramolecular exchange coupling exceeds the order of a thermal energy around 300 K. Measurements on lowering temperature displayed a monotonic $\chi_m T$ decrease, being assignable to intermolecular antiferromagnetic interaction. In short, the spin structure is depicted as ⋯↑↑⋯↓↓⋯↑↑⋯↓↓⋯.

Another morph was found for BPBN and 25MeBPBN, which was structurally and magnetically characterized and named as the α-phase. The $\chi_m T$ values were null below ca. 350 K for α-BPBN [21] and α-25MeBPBN [22], indicating complete loss of spins. The biradical revived in solution, as clarified by means of EPR spectroscopy. A solution SQUID magnetometry confirmed the triplet ground state of each molecule. On heating the polycrystalline specimens of α-BPBN and α-25MeBPBN, the $\chi_m T$ values showed an abrupt jump to 0.95 cm^3 K mol^{-1}. The transition temperatures are 350 and 360 K, respectively. The transitions were irreversible, as shown in measurements with repeated thermal cycles. The powder XRD study clarified that this transition did not involve melt but solid-state/solid-state structural transition. The single-crystal structural analysis indicates that the α- and β-phases can be regarded as polymerized and depolymerized forms, respectively (see below).

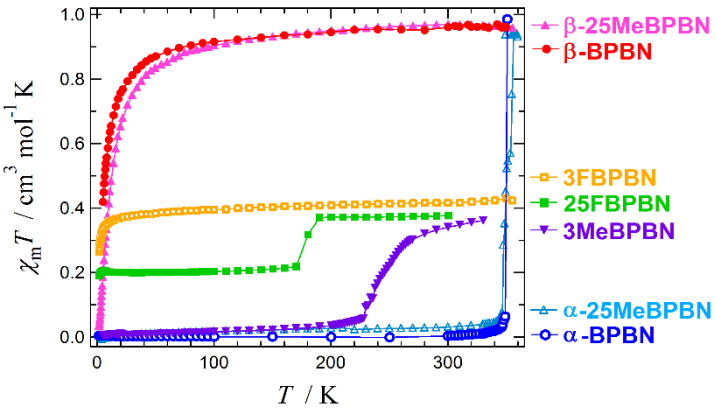

Figure 2. Magnetic study results on BPBN derivatives.

A half level of the $\chi_m T$ value (ca. 0.40 cm^3 K mol^{-1}) was recorded for 3FBPBN [23], being close to the theoretical level typical of S = 1/2 species (0.38 cm^3 K mol^{-1}) (Figure 2). As the crystallographic analysis of 3FBPBN clarified (see below), one hand participates in dimerization while the other remains free. As a result, two residual spins come from every four spins.

The $\chi_m T$ vs T curve of 3MeBPBN [24] (Figure 2) displayed a gradual spin transition. A practically diamagnetic feature appeared in the LT phase. On heating, the $\chi_m T$ value started a monotonic increase from ca. 230 K and reached to an approximate plateau at 0.35 cm^3 K mol^{-1} around 300 K in the HT phase, which corresponds to the theoretical S = 1/2 value. The interconversion was reversible. Thermochromism was also observed; the LS and HS phases are orange and red, respectively.

More interestingly, a reversible, abrupt and hysteretic spin transition was found at $T_{C\uparrow}$ = 182 K on heating and $T_{C\downarrow}$ = 181 K on cooling for 25FBPBN [23] (Figure 2). The transition was completed in a width of ca. 3 K. In the HT phase, the $\chi_m T$ value is close to the S = 1/2 theoretical value, just like 3FBPBN. Most interestingly, a quarter level of the total spin amount ($\chi_m T$ = ca. 0.20 cm^3 K mol^{-1}) was recorded in the LT phase.

(a)

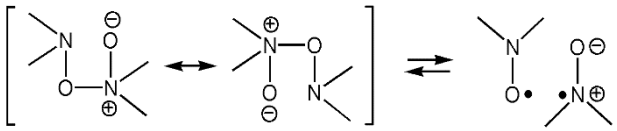

(b)

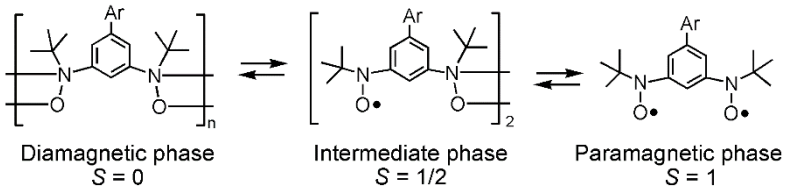

Scheme 3. (a) Equilibrium of covalent-bond/radical-pair forms. (b) Three phases of a linear array: polymer (left), dimer (center), and monomer (right) on the BPBN-molecular basis.

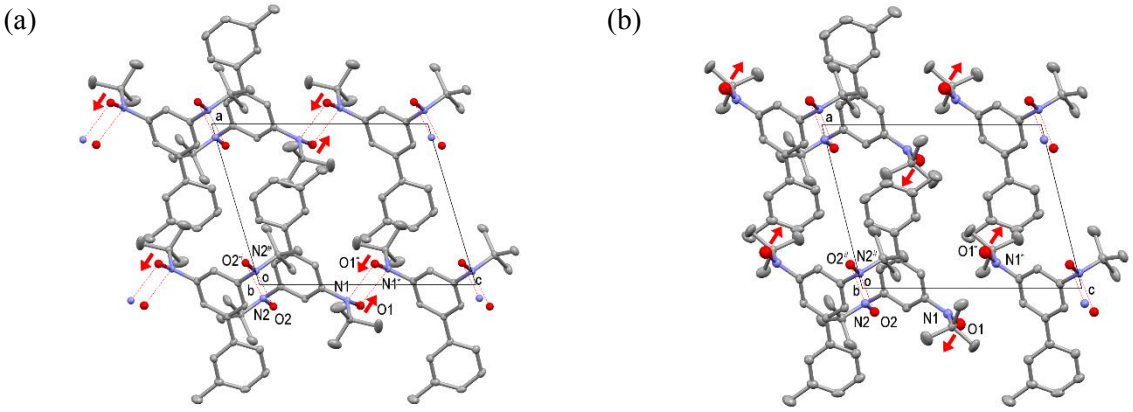

Figure 3. Crystal structures of 3MeBPBN at 116 K (a) and 296 K (b). Hydrogen atoms are omitted for clarity. Moving groups are marked with small arrows, and short contacts with dotted lines. Molecules are linearly arrayed in a crystallographic $b + c$ diagonal direction. The intermolecular N1···O1' distances are 2.379(2) and 3.686(3) Å at 116 and 296 K, respectively.

Detailed crystallographic analysis perfectly explains all the magnetic properties. The molecules are linearly arrayed with each nitroxide group closely interacted in an intermolecular fashion (Scheme 3). The intramolecular ferromagnetic and intermolecular antiferromagnetic couplings are simultaneously present and competing in a chain-like molecular arrangement. Figure 3 shows the result on 3MeBPBN [24]. The intermolecular interaction is overwhelmingly stronger than the intramolecular interaction in the LT phase. The crystallographic inversion center of the $P\bar{1}$ space group is located at the midpoint of a head-to-tail $(N\text{-}O)_2$ motif (Scheme 3a). Such a dimerization mode is reasonable from the canonical dipolar structure $>N^{+\bullet}\text{-}O^{-}$, and similar arrangements have been well known [26–28]. The peroxide-type O-O bond is rather rare [29], in good agreement with the thermodynamic consideration [30,31]. The N-O radical groups are separated from each other by 2.3 - 2.4 Å for O···N at 116 K, being considerably shorter than the sum of the van der Waals radii (O/N: 3.07 Å [32]). Therefore, the molecular structure can be well described as a diamagnetic phase or covalent polymer (Scheme 3b, left). At 296 K (Figure 3b), the O1···N1 separation becomes further whereas the O2···N2 proximity still remains. According to the classification of the phases, the resultant linear array belongs to the intermediate paramagnetic form (Scheme 3b, center). Transient structures could be tracked at any temperature, and the result of the variable-temperature crystallographic study has been deposited as an animated picture file at the electronic supporting information (ESI) site [24]. A very gradual structure transition was recorded.

Note that the present spin transition could not be analyzed according to the conventional spin equilibrium such as a singlet-triplet (Bleaney-Bowers) model [33]. During the transition, the atoms are dislocated, the molecules are deformed, and the exchange coupling is not constant. In other words, this situation is best described as a solid-state reaction. A chemical equilibrium occurs between covalent bond and radical-pair forms.

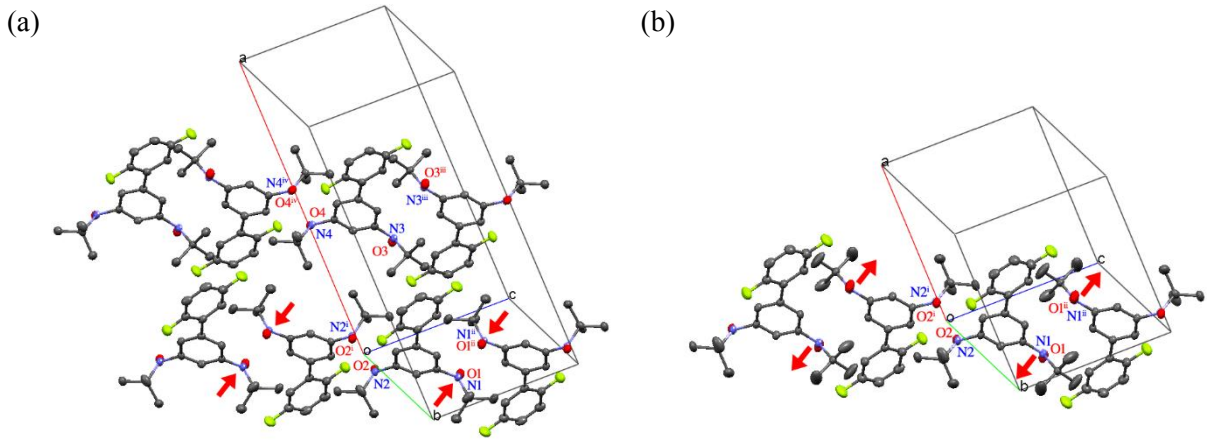

Figure 4. Crystal structures of 25FBPBN at 100 K (a) and 296 K (b). Hydrogen atoms are omitted for clarity. Moving groups are marked with small arrows. The intermolecular N1···O1^{ii} distances are 2.425(4) and 3.696(4) Å at 100 and 296 K, respectively. Molecules are linearly arrayed in a crystallographic $b + c$ diagonal direction.

The crystallographic analysis on 25FBPBN [23] (Figure 4) clarifies that 3/4 of spins (N1-O1, N2-O2, and N4-O4) are strongly dimerized at 100 K whereas 1/2 of spins (N2-O2) is dimerized at 296 K, just like the HT phase of 3MeBPBN (Figure 3b). The HT form corresponds to the intermediate phase in Scheme 3b. The chains are differentiated on lowering temperature. Across T_C one chain became a diamagnetic polymer (Scheme 3b, left), while the other maintained the intermediate structure (Scheme 3b, center). In short, the asymmetric cell is doubled in the LT phase. Two spins survive from every eight spins. Transient structures could be monitored, and the result of the variable-temperature crystallography has been deposited as an animated picture file at the ESI site [23].

The crystal structures are classified into a few phases on the basis of the paramagnetic properties or the amount of paramagnetic portions. The HT phase of 3MeBPBN (Figure 3b) is isomorphous to that of 3FBPBN and also to that of the HT phase of 25FBPBN. The LT phase of 3MeBPBN (Figure 3a) is isomorphous to those of α-BPBN and α-25MeBPBN.

An abrupt and hysteretic character of spin transition attracts attention toward future application. Since 25FBPBN displayed a thermal hysteresis, this transition is described as a first-order phase transition. A single-crystal-to-single-crystal transition was still realized here. The relatively small enthalpy change may allow gradual dislocation of moving groups in 25FBPBN. The long-range interaction doubling the unit cell seems to be responsible for the cooperativity [34] as well as the structural phase transition as a bulk phenomenon.

One may wonder possibility of the radical dimerization in solution. Preorganization generally reduces the entropy loss during dimerization. Actually we designed and attempted to prepare pincer-type bisnitroxide compounds, in which the paramagnetic centers are forced to be closely located in a molecule [35]. This technique has been applied to triphenylimidazolyl compounds, and thermo-/photochromism has been successfully demonstrated [36,37].

In summary, the solid BPBN family affords a rare opportunity, where boundary zones are observable between chemical equilibrium and phase transition and between strong antiferromagnetic coupling and weak chemical bonding.

3. Spin transition materials from 3d-2p heterospin systems

Frontier-orbital engineering is a versatile concept for materials science. Heterospin approaches utilize the wide diversity of the characteristic features including the symmetry and energy level of magnetic orbitals [38]. The metal-radical approach afforded fruitful results [39]. In particular, a paramagnetic

center – typically nitroxide – oxygen atom is directly bonded to a metal center, leading to considerably strong exchange coupling.

Copper(II)- and nickel(II)-radical complexes are best described in the 3d-2p-bonded heterospin compounds [40,41]. Axial coordination in Cu^{2+}-nitroxide complexes is known to exhibit relatively weak ferromagnetic interaction, whereas equatorial coordination results in strong antiferromagnetic interaction [39]. However, from more recent related studies, ferromagnetic interaction is available as well from equatorial coordination (Figure 5) [40–46]. The magnitudes of the exchange couplings often are higher than the order of a thermal energy around 300 K, whether antiferro- or ferromagnetic. The author and co-workers have proposed the torsion angle ϕ around M-O-N-Cα as a convenient and useful metric to evaluate the planarity of the coordination structure and furthermore orthogonality of the magnetic orbitals [47,48]. There has been no report on the magneto-structure relationship on 3d-2p heterospin coordination compounds before the present project.

When the coordination structure is coplanar between the metal coordination plane and radical π-conjugation plane (i.e., $|\phi|$ is small), ferromagnetic coupling is dominant. Five-membered chelate rings are more favorable for planar coordination structure than six-membered ones. Thus, 2-pyridyl nitroxide derivatives are supposed to be promising [14–16,45–51]. Ferromagnetic coupling is afforded when two magnetic orbitals (π* and dσ) are arranged in a strictly orthogonal manner (Figure 6a,c). In contrast, severe twist deformation around the coordination bond brings about an appreciable overlap between the magnetic orbitals, giving antiferromagnetic coupling (Figure 6b,d). The critical $|\phi|$, at which the sign of the metal-radical exchange coupling changes from positive to negative, is 12.5(8)° [47,48]. After the data on the Cu^{2+} and Ni^{2+} complexes are separated, the critical angle for Ni^{2+} complexes was refined to be 21(1)° from the linear fit or 26(3)° from the $\cos^2\phi$ fit [52]. The plot of exchange coupling vs torsion is also competently utilized to 4f-2p heterospin systems afterward [53–56].

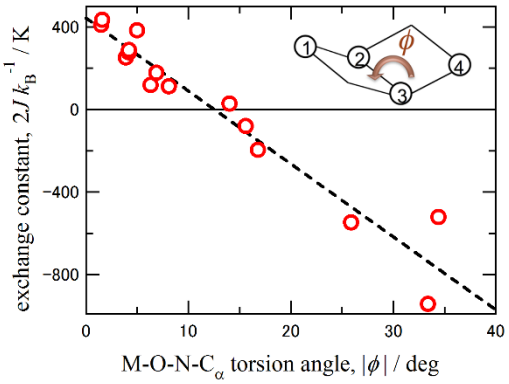

Figure 5. Plot of the exchange coupling parameter (J) vs M-O-N-Cα torsion angle ($|\phi|$) in the Cu^{2+} and Ni^{2+} complexes with paramagnetic ligands. Inset shows a schematic drawing of ϕ defined along atoms 1-2-3-4.

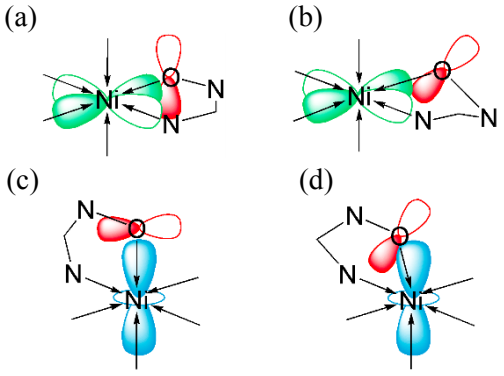

Figure 6. Mutual geometries between Ni^{2+} (or Cu^{2+}) $3d_{x^2-y^2}$ and $O_{nitroxide}$ $2p_z$ (a,b) and between Ni $3d_{z^2}$ and $O_{nitroxide}$ $2p_z$ (c,d).

Now, upon these backgrounds, the author describes here a heterospin 2p-3d-2p triad $[M(L)_2X_2]$ showing a novel SCO behavior. Actually, a series of $[Ni(phpyNO)_2X_2]$ was prepared (phpyNO = *tert*-butyl 5-phenyl-2-pyridyl nitroxide [47]) (Scheme 4). After complex formation, the stability under ambient conditions is much improved. Analogues with X = Cl and Br displayed SCO, and those with X = NCO, NCS, and NCSe an indication of SCO [57,58]. The following description is focused on the X = Cl derivative [57].

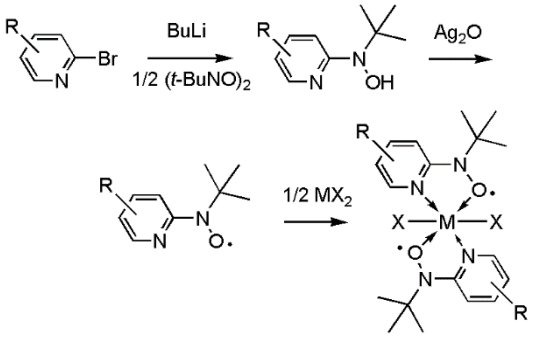

Scheme 4. Synthetic route to double chelates from 2-pyridyl nitroxides.

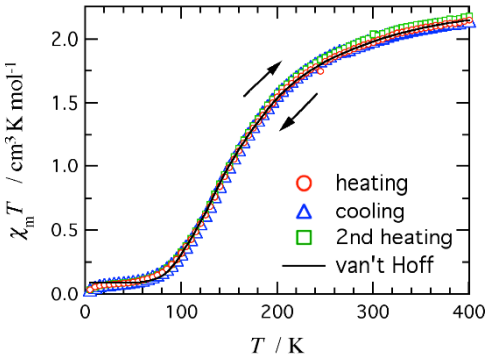

Figure 7. Temperature dependence of $\chi_m T$ for $[Ni(phpyNO)_2Cl_2]$. Temperature scan sequence is also indicated.

As the magnetic susceptibility measurements clarify (Figure 7), the $\chi_m T$ value of $[Ni(phpyNO)_2Cl_2]$ was 2.14 cm^3 K mol^{-1} and still showed a slope at 400 K. An estimated high-temperature value is 2.38(2) cm^3 K mol^{-1}, being larger than the paramagnetic (noninteracting) limit. This finding implies that the ferromagnetic coupling is observable even at room temperature. The spin structure is drawn as ↑-↑↑-↑. With a decrease of temperature, the $\chi_m T$ value exhibited a monotonic and dramatic decrease, indicating the presence of notable antiferromagnetic interaction. The spin structure becomes ↓-↑↑-↓. Therefore, the present compound underwent a spin switch between the ground states of $S_{total} = 2$ and 0. No thermal hysteresis was recorded.

From the crystallographic analysis on $[Ni(phpyNO)_2Cl_2]$, the Ni^{2+} ion forms an octahedral geometry, guaranteeing the HS Ni^{2+} ion ($S_{Ni2+} = 1$). Two nitroxide groups are arranged in a *cis* position. On cooling to 85 K, the space group $P2_1/c$ was unchanged, and the Ni-O1, Ni-O2, and other interatomic distances were practically unchanged either. In contrast, both Ni-O-N-C$\alpha_{(2py)}$ torsion angles drastically increased, as shown in Figure 8. They seem to go across the critical $|\phi|$. The breakdown of the d-π* orthogonal arrangement leads to antiferromagnetic interaction on cooling. An animated picture file has been deposited with ESI [57], visualizing a very gradual bond twisting.

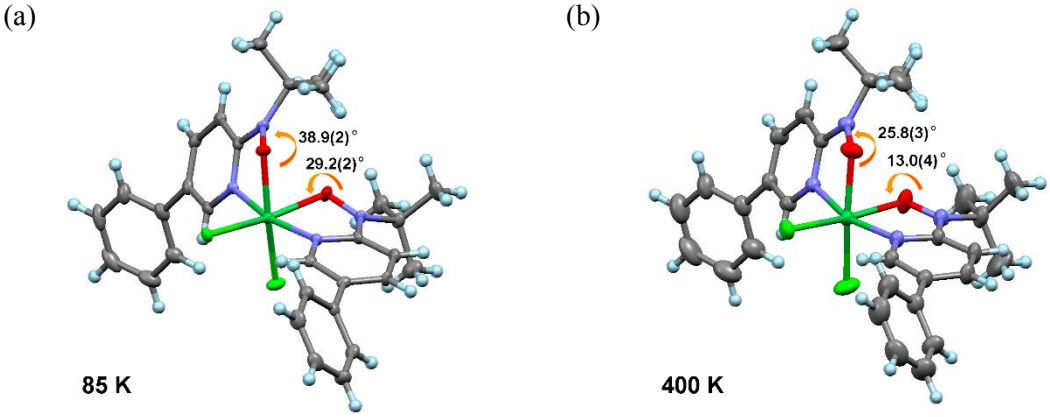

Figure 8. X-ray crystal structures of $[Ni(phpyNO)_2Cl_2]$ measured at 85 K (a) and 400 K (b). Ni-O-N-C$\alpha_{(2py)}$ torsion angles are indicated.

From the thermodynamic point of view, the magnetic data were found to perfectly obey the van't Hoff equation (Figure 7), which has been proposed to comprehend SCO behavior [34]. The entropy change of the phase transition was calculated to be $\Delta S = 26.3(1)$ J K^{-1} mol^{-1} from the equation $\Delta G =$

$\Delta H - T\Delta S = 0$. The entropy gain due to the spin multiplicity is R ln 5 = 13.4 J K^{-1} mol^{-1}. An additional entropy change is suggested, and the HT form is supposed to include other degrees of freedom such as vibration [3,34]. A single-crystal-to-single-crystal structural transition was realized. It is because the spin entropy term regulates the atomic dislocation enthalpy, and the entropy change due to the spin multiplicity is basically small. Thus, the thermodynamic consideration is entirely consistent with the magnetic and structural discussion. The two Ni-O-N-C$\alpha_{(2py)}$ twists are synchronized. Both interactions change from ferromagnetic to antiferromagnetic with a decrease of temperature, because the spin multiplicity should be minimized (S_{total} = 0).

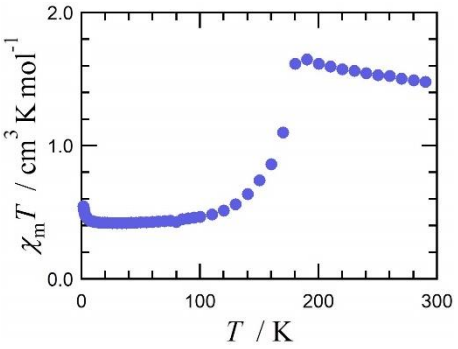

Figure 9. $\chi_m T$ vs T plot for [Cu(phpyNO)$_2$(H$_2$O)$_2$](BF$_4$)$_2$.

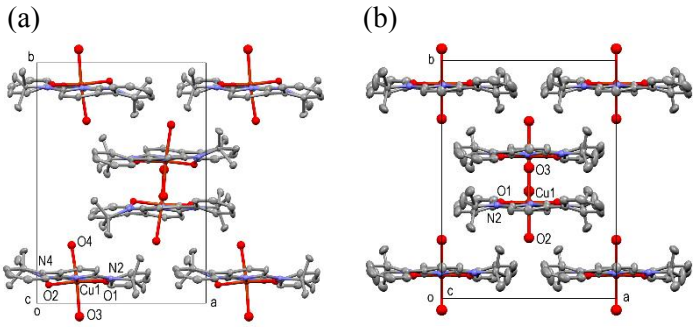

Figure 10. Molecular arrangements at 94 K (a) and 204 K (b) for [Cu(phpyNO)$_2$(H$_2$O)$_2$](BF$_4$)$_2$. Counter anions and hydrogen atoms are omitted. The space groups are $P2_12_12_1$ and $C222_1$ at 94 and 204 K, respectively.

The results on the corresponding copper(II) complexes confirm this notion. Applying a copper(II) ion source to a general synthesis (Scheme 4) gave a complex salt [Cu^{II}(phpyNO)$_2$(H$_2$O)$_2$](BF$_4$)$_2$ [59]. In a HT region, the magnetic study clarifies the presence of the ferromagnetic coupling on both sides (Figure 9); namely, the spin structure was drawn as ↑-↑-↑ to give S_{total} = 3/2. In a LT region, the $\chi_m T$ value indicates S_{total} = 1/2. The ground S_{total} = 1/2 state is given, regardless of antiferromagnetic interaction operative on either side or both. The crystallographic analysis reveals that the exchange switch took place around 175 K only on one side (Figure 10). A chelate ring underwent out-of-plane deformation, leading to loss of a molecular/crystalline symmetry element. Thus, the spin structure is written as ↑-↑-↓ and not ↑-↓-↑. No synchronous switch is necessary in this case. Despite the sharp $\chi_m T$ drop with a decrease of temperature, the specimen retained a single-crystalline form. An animated picture file has been deposited with ESI [59].

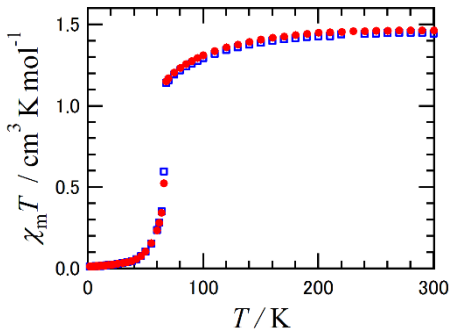

Figure 11. $\chi_m T$ vs T plot for [Cu^{2+}(2pyNO•)(2pyNO$^-$)]$_2$(BF$_4^-$)$_2$.

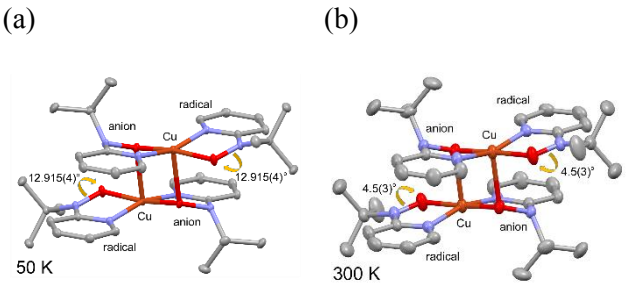

Figure 12. Molecular structures at 50 K (a) and 300 K (b) for [Cu^{2+}(2pyNO•)(2pyNO$^-$)]$_2$(BF$_4^-$)$_2$. Counter anions and hydrogen atoms are omitted.

Another complex has been investigated with a M/L(radical) ratio of 1/1. Applying 2pyNO and the corresponding diamagnetic hydroxylamine to copper(II) complex formation with a molar ratio 1/1/1, $[Cu^{2+}(2pyNO\bullet)(2pyNO^{-})]_2(BF_4^{-})_2$ was obtained [60]. The anionic oxygen atom bridges a nearest Cu^{2+} ion at the axial position. Although a four-centered system was formed, the magnetic system can approximately be regarded as a two-centered system. As Figure 11 shows, a relatively abrupt spin transition occurs at 64 K; the spin structures are drawn as ↑-↑ for the HT phase and ↑-↓ for the LT phase for all the paramagnetic portions. In this case, to achieve the LS state as a whole molecule, all the chelate rings are synchronously deformed (Figure 12).

After combining the results on the above Ni^{2+}- and Cu^{2+}-nitroxide complexes, it can be concluded that the SCO is entropy-driven, i.e., driven under the control of the spin entropy. The spin triads or dyads exhibited a thermally induced SCO on the whole heterospin molecular basis, in which the exchange coupling is converted between ferro- and antiferromagnetic. Owing to the slight molecular motion like inner conformational change, the single-crystal nature was kept during the transition. As seen in several complexes described above, such novel SCO materials are not so rare in multi-centered 3d-2p heterospin compounds. The present work expands a concept of SCO and will open potential application taking advantage of possible wide derivatization of organic and counterion portions.

As a closely related system, the following study should be referred. Ovcharenko et al. reported the spin-transition materials in Cu^{2+}-nitroxide complexes [61,62]. This mechanism involves a switch of the role of axial and equatorial coordination sites and works only for Cu^{2+} systems. In contrast, author's group focused on octahedral Ni^{2+} complexes as well, in which a coupling switch actually occurred regardless of the coordination positions. In other words, the mechanism proposed here may be broadly applied to complexes carrying dσ spins. Another advantage of the present system is the inclusion of room-temperature-class strong ferromagnetic coupling in the HT structure.

4. Spin transition materials from 3d systems

Multifunctional SCO substances toward future application attract much attention to materials chemists; for example, SCO with magnetic exchange coupling [63–65] and with mesophase or liquid crystal properties seems to be fascinating [66–71]. Iron(II) ($3d^6$) complexes are supposed to be the most important family of SCO compounds. HS states tend to have longer metal-ligand bonds than LS states [1–4], and this inevitably means that the molecular and crystal structures are deformed during SCO. Thus, the detailed SCO study has often clarified various phase transition modes like stepwise, hysteretic, incomplete, etc., which might be overlooked only from the viewpoint of the structural chemistry. Symmetry-breaking SCO has often been characterized with the stepwise thermal hysteresis [68,72].

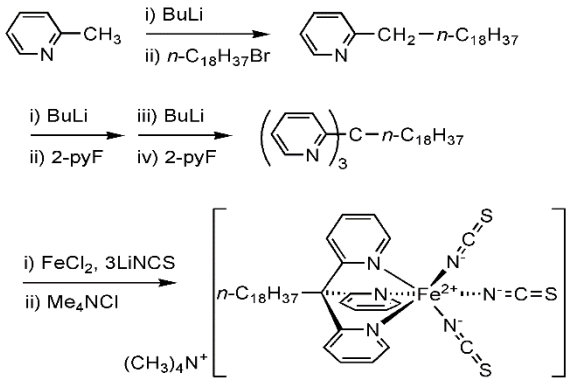

Scheme 5. Synthetic route to $Me_4N[Fe(L^{C18})(NCS)_3]$.

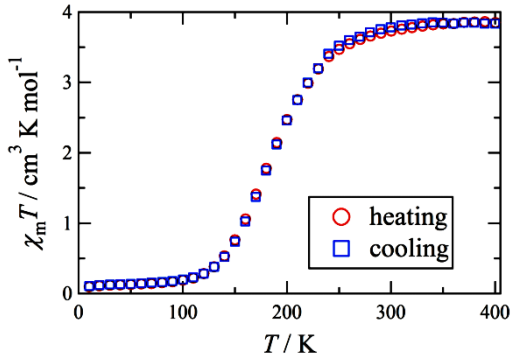

Figure 13. Temperature dependence of $\chi_m T$ for $Me_4N[Fe(L^{C18})(NCS)_3]$, measured on heating and then cooling.

In this work a stearyl-substituted ligand (abbreviated as L^{C18}) has been designed as a polymorphic SCO ligand prototype. The target compound, $Me_4N[Fe(L^{C18})(NCS)_3]$ [73], was synthesized according to Scheme 5. The specimen possesses no solvent molecule. It seems to be noticeable that anionic SCO complex ions $[Fe(L^X)(NCS)_3]^-$ (X = H, CH_3, OH, 2-pyridyl, OCH_3) are uncommon [74–79]. The magnetic susceptibility of $Me_4N[Fe(L^{C18})(NCS)_3]$ was measured up to 400 K, and the $S = 0 \rightleftarrows 2$ SCO occurred in a one-step and nonhysteretic manner, as Figure 13 demonstrates.

The X-ray crystallographic analysis on $Me_4N[Fe(L^{C18})(NCS)_3]$ was performed between 100 and 300 K; these temperatures correspond to just below and above the SCO range (Figure 14). A layered structure is constructed with the layer distance of 30.5 Å. A gauche conformation is found at the fourth single bond in the chain, and all other carbon atoms are arranged in anti zigzag conformation. At 300 K, the space group is $P2_1/c$ with $Z = 4$, and there is a crystallographically unique ion pair Me_4N^+ $[Fe(L^{C18})(NCS)_3]^-$ in a unit cell (Figure 14b). At 100 K, the crystal symmetry was lowered to give a space group $P\bar{1}$ with $Z = 4$, and there are two independent units (Figure 14a). The torsion angles around the fourth single bond in the chain are differentiated to be 58.8(7) and 63.7(7)°.

However, interestingly, the two conformers synchronously underwent SCO, as clarified with the X-ray structural analysis on transient crystals. It seems to be a very rare case, where the SCO profile is gradual, one-step, and nonhysteretic, despite the change in the crystal system and space group [68,72,80–84]. The gauche conformation appears for minimization of the crystal void space. In this context, to maintain a commensurate bilayer structure, the gauche angle is deviated. Accordingly, the SCO is supposed to cause the structural change.

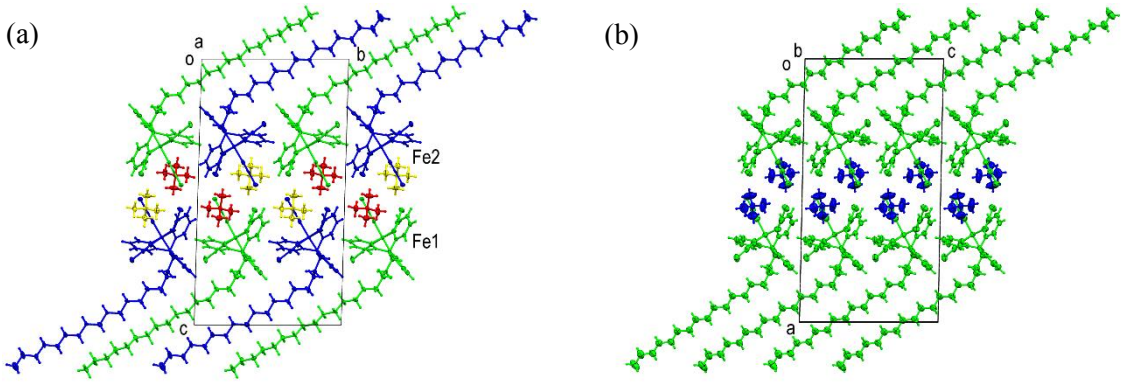

Figure 14. X-ray crystal structures of $Me_4N[Fe(L^{C18})(NCS)_3]$ measured at 100 K (a) and 300 K (b). Crystallographically independent molecules are colored by symmetry equivalence.

In summary, $Me_4N[Fe(L^{C18})(NCS)_3]$ underwent SCO with a considerably gradual order-disorder-type structural transition. The transition temperature range is as wide as ca. 200 K. An organic flexible group was elaborately introduced, and the polymorphic transition is successfully materialized.

5. Conclusion

The three types of spin transition materials consisting of 2p spin, 3d-2p heterospin, and 3d spin systems have been described, and the corresponding magneto-structure relationships have been discussed in detail on the basis of the molecular deformation observed. In fact, we encounter molecular motion in crystalline solids more frequently than expected! Such molecular motion can be monitored by means of attentive crystallographic study, thus affording one of the most convincing evidence for the spin transition phenomenon. As seen above, author's group has developed various unconventional spin transition materials.

The molecules and crystals are gradually transformed in a wide temperature range, and the present solid-state/solid-state structural transition – or more correctly, structure crossover – involves only a small geometrical change. A single-crystal-to-single-crystal structural transformation would be

welcomed for crystallographic study, and such favorable conditions are often realized. It is inevitable rather than accidental. It is because paramagnetic centers move in crystals to satisfy thermodynamic conditions. The spin entropy term regulates the enthalpy term leading to minimal atomic dislocation, i.e., $T_{1/2}\Delta_{tr}S = \Delta_{tr}H$, and the entropy change due to the spin multiplicity is basically small.

Since the molecules are transformed through solid-state chemical reactions, intersystem crossing, and/or conformational isomerization, the physical properties must concomitantly change, including conductivity, dielectricity, elasticity, chromism as well as magnetism. Among the vast variation of SCO compounds, there are instances showing an abrupt transition and sometimes thermal hysteresis (Figures 2, 9, 11), being suitable for future application to smart devices. Application-oriented research is a next challenge.

References

[1] Gütlich P and Goodwin H A 2004 *Spin Crossover in Transition Metal Compounds I, II and III* (Berlin Heidelberg: Springer-Verlag)
[2] Halcrow M A 2013 *Spin-Crossover Materials: Properties and Applications* (Chichester, West Sussex, United Kingdom: Wiley)
[3] Kahn O 1993 *Molecular magnetism* (New York, NY: VCH)
[4] Senthil Kumar K and Ruben M 2017 Emerging trends in spin crossover (SCO) based functional materials and devices *Coordination Chemistry Reviews* **346** 176–205
[5] Gentili D, Demitri N, Schäfer B, Liscio F, Bergenti I, Ruani G, Ruben M and Cavallini M 2015 Multi-modal sensing in spin crossover compounds *Journal of Materials Chemistry C* **3** 7836–44
[6] Hicks R 2011 *Stable radicals: fundamentals and applied aspects of odd-electron compounds* (John Wiley & Sons)
[7] Iwamura H 2013 What role has organic chemistry played in the development of molecule-based magnets? *Polyhedron* **66** 3–14
[8] Mukai K and Tamaki T 1978 Synthesis and magnetic properties of stable crystalline *p*-phenylenebis(galvinoxyl) biradical *The Journal of Chemical Physics* **68** 2006–7
[9] Calder A, Forrester A R and Thomson R H 1969 Nitroxide radicals. Part IV. The oxidation of cyclic N-hydroxy-imides *Journal of the Chemical Society C: Organic* 512
[10] Ishida T and Iwamura H 1991 Bis[3-tert-butyl-5-(N-oxy-tert-butylamino)phenyl] nitroxide in a quartet ground state: a prototype for persistent high-spin poly[(oxyimino)-1,3-phenylenes] *Journal of the American Chemical Society* **113** 4238–41
[11] Lahti P M 2011 Structure–property relationships for metal-free organic magnetic materials *Advances in Physical Organic Chemistry* vol 45 (Elsevier) pp 93–169
[12] Matsumoto T, Ishida T, Koga N and Iwamura H 1992 Intramolecular magnetic coupling between two nitrene or two nitroxide units through 1,1-diphenylethylene chromophores. Isomeric dinitrenes and dinitroxides related in connectivity to trimethylenemethane, tetramethyleneethane, and pentamethylenepropane *Journal of the American Chemical Society* **114** 9952–9
[13] Yoshitake T and Ishida T 2016 Ferromagnetic Chains of Ground Triplet 5-Methoxy-1,3-phenylene Bis(*tert*-butyl nitroxide) *Chemistry Letters* **45** 391–3
[14] Homma Y, Okazawa A and Ishida T 2013 Ground triplet pyrimidine-4,6-diyl bis(tert-butyl nitroxide) as a paramagnetic building block for metal–organic frameworks *Tetrahedron Letters* **54** 3120–3
[15] Kawakami H, Tonegawa A and Ishida T 2016 A designed room-temperature triplet ligand from pyridine-2,6-diyl bis(tert-butyl nitroxide) *Dalton Transactions* **45** 1306–9
[16] Kawakami H, Tonegawa A and Ishida T 2016 Pyridine-2,6-diyl dinitroxides as room-temperature triplet ligands The Irago Conference 2015: A 360 Degree Outlook on Critical Scientific and Technological Challenges for a Sustainable Society (Aichi, Japan) *AIP Conference Proceedings* **1709**, 020017

[17] Iwahori F, Inoue K and Iwamura H 1999 Mn(II)-Induced Formation and Structural Elucidation of a [3+3] Benzene Dimer Derivative from *m*-Phenylenebis(N-tert-butylaminoxyl) *Journal of the American Chemical Society* **121** 7264–5
[18] Sekine H and Ishida T 2018 Unexpected complexes from meta-phenylene bis(tert-butyl nitroxides) and gadolinium(III) 1,1,1,5,5,5-hexafluoropentane-2,4-dionate The Irago Conference 2017: A 360-degree Outlook on Critical Scientific and Technological Challenges for a Sustainable Society (Tokyo, Japan) *AIP Conference Proceedings* **1929** 020022
[19] Sekine H and Ishida T 2018 Unexpected Complexes of a [3+3] Cycloadduct from Biphenyl-3,5-diyl Bis(tert-butyl nitroxide) with Gadolinium(III) 1,1,1,5,5,5-Hexafluoropentane-2,4-dionate *Chemistry Letters* **47** 74–7
[20] Kurokawa G, Ishida T and Nogami T 2004 Remarkably strong intermolecular antiferromagnetic couplings in the crystal of biphenyl-3,5-diyl bis(tert-butyl nitroxide) *Chemical Physics Letters* **392** 74–9
[21] Nishimaki H, Mashiyama S, Yasui M, Nogami T and Ishida T 2006 Bistable Polymorphs Showing Diamagnetic and Paramagnetic States of an Organic Crystalline Biradical Biphenyl-3,5-diyl Bis(*tert*-butylnitroxide) *Chemistry of Materials* **18** 3602–4
[22] Yoshitake T, Kudo H and Ishida T 2016 Thermally Activated Paramagnets from Diamagnetic Polymers of Biphenyl-3,5-diyl Bis(tert-butyl Nitroxides) Carrying Methyl and Fluoro Groups at the 2'- and 5'-Positions *Crystals* **6** 30
[23] Konno T, Kudo H and Ishida T 2015 Intermediate-paramagnetic phases with a half and a quarter spin entities in fluorinated biphenyl-3,5-diyl bis(tert-butyl nitroxides) *Journal of Materials Chemistry C* **3** 7813–8
[24] Nishimaki H and Ishida T 2010 Organic Two-Step Spin-Transition-Like Behavior in a Linear *S* = 1 Array: 3′-Methylbiphenyl-3,5-diyl Bis(*tert*-butylnitroxide) and Related Compounds *Journal of the American Chemical Society* **132** 9598–9
[25] Suzuki A 2011 Cross-Coupling Reactions Of Organoboranes: An Easy Way To Construct C–C Bonds (Nobel Lecture) *Angewandte Chemie International Edition* **50** 6722–37
[26] Matsumoto S, Higashiyama T, Akutsu H and Nakatsuji S 2011 A Functional Nitroxide Radical Displaying Unique Thermochromism and Magnetic Phase Transition *Angewandte Chemie International Edition* **50** 10879–83
[27] Capiomont A, Chion B and Lajzérowicz J 1971 Affinement de la structure du radical nitroxyde dimerisé: bicyclo[3,3,l]nonanone-3 aza-9 oxyle-9 *Acta Crystallographica Section B Structural Crystallography and Crystal Chemistry* **27** 322–6
[28] Ishida T, Ooishi M, Ishii N, Mori H and Nogami T 2007 Mono- and dinitroxide radicals from 9,9′(10H,10′H)-spirobiacridine: An approach to a D_{2d} triplet biradical *Polyhedron* **26** 1793–9
[29] Kanetomo T and Ishida T 2017 Notably Strong Antiferromagnetic Interaction in a Methylene-bridged Bis(dihydrophenanthridin-*N*-oxyl) *Chemistry Letters* **46** 188–90
[30] Keana J F W 1978 Newer aspects of the synthesis and chemistry of nitroxide spin labels *Chemical Reviews* **78** 37–64
[31] Bowman D F, Gillan T and Ingold K U 1971 Kinetic applications of electron paramagnetic resonance spectroscopy. III. Self-reactions of dialkyl nitroxide radicals *Journal of the American Chemical Society* **93** 6555–61
[32] Bondi A 1964 van der Waals Volumes and Radii *The Journal of Physical Chemistry* **68** 441–51
[33] Bleaney B and Bowers K D 1952 Anomalous Paramagnetism of Copper Acetate *Proceedings of the Royal Society A: Mathematical, Physical and Engineering Sciences* **214** 451–65
[34] Boča R 1999 *Theoretical foundations of molecular magnetism* vol 1 (Elsevier)
[35] Koizumi N and Ishida T 2017 Forced proximity of nitroxide groups in pincer compounds with a xanthene spacer *Tetrahedron Letters* **58** 2804–8
[36] Kishimoto Y and Abe J 2009 A Fast Photochromic Molecule That Colors Only under UV Light *Journal of the American Chemical Society* **131** 4227–9

[37] Hatano S, Horino T, Tokita A, Oshima T and Abe J 2013 Unusual Negative Photochromism via a Short-Lived Imidazolyl Radical of 1,1′-Binaphthyl-Bridged Imidazole Dimer *Journal of the American Chemical Society* **135** 3164–72
[38] Miller J S and Gatteschi D 2011 Molecule-based magnets *Chemical Society Reviews* **40** 3065
[39] Caneschi A, Gatteschi D, Sessoli R and Rey P 1989 Toward molecular magnets: the metal-radical approach *Accounts of Chemical Research* **22** 392–8
[40] Luneau D, Rey P, Laugier J, Fries P, Caneschi A, Gatteschi D and Sessoli R 1991 Nitrogen-bonded copper(II)-imino nitroxide complexes exhibiting large ferromagnetic interactions *Journal of the American Chemical Society* **113** 1245–51
[41] Luneau D, Rey P, Laugier J, Belorizky E and Cogne A 1992 Ferromagnetic behavior of nickel(II)-imino nitroxide derivatives *Inorganic Chemistry* **31** 3578–84
[42] Aoki C, Ishida T and Nogami T 2003 Metamagnetic behavior of $[Ni(4ImNNH)_2(NO_3)_2]$ having a ground high-spin state (4ImNNH = 4-imidazolyl nitronyl nitroxide) *Inorganic Chemistry Communications* **6** 1122–5
[43] Aoki C, Ishida T and Nogami T 2003 Molecular Metamagnet $[Ni(4ImNNH)_2(NO_3)_2]$ (4ImNNH = 4-Imidazolyl Nitronyl Nitroxide) and the Related Compounds Showing Supramolecular H-Bonding Interactions *Inorganic Chemistry* **42** 7616–25
[44] Yamamoto Y, Suzuki T and Kaizaki S 2001 Syntheses, structures, magnetic, and spectroscopic properties of cobalt(ii), nickel(ii) and zinc(ii) complexes containing 2-(6-methyl)pyridyl-substituted nitronyl and imino nitroxide *Journal of the Chemical Society, Dalton Transactions* 2943–50
[45] Osanai K, Okazawa A, Nogami T and Ishida T 2006 Strong Ferromagnetic Exchange Couplings in Copper(II) and Nickel(II) Complexes with a Paramagnetic Tridentate Chelate Ligand, 2,2'-Bipyridin-6-yl *tert*-Butyl Nitroxide *Journal of the American Chemical Society* **128** 14008–9
[46] Okazawa A, Nogami T and Ishida T 2007 tert-Butyl 2-Pyridyl Nitroxide Available as a Paramagnetic Chelate Ligand for Strongly Exchange-Coupled Metal−Radical Compounds *Chemistry of Materials* **19** 2733–5
[47] Okazawa A, Nagaichi Y, Nogami T and Ishida T 2008 Magneto-Structure Relationship in Copper(II) and Nickel(II) Complexes Chelated with Stable tert-Butyl 5-Phenyl-2-pyridyl Nitroxide and Related Radicals *Inorganic Chemistry* **47** 8859–68
[48] Okazawa A, Nogami T and Ishida T 2009 Strong intramolecular ferromagnetic couplings in nickel(II) and copper(II) complexes chelated with tert-butyl 5-methoxy-2-pyridyl nitroxide *Polyhedron* **28** 1917–21
[49] Okazawa A, Terakado Y, Ishida T and Kojima N 2018 A triplet biradical with double bidentate sites based on tert-butyl pyridyl nitroxide as a candidate for strong ferromagnetic couplers *New Journal of Chemistry* **42** 17874-78
[50] Konno T, Koide K and Ishida T 2013 A supramolecular switch between ground high- and low-spin states using 2,2′:6′,2″-terpyridine-6,6″-diyl bis(tert-butyl nitroxide) *Chemical Communications* **49** 5156
[51] Koide K and Ishida T 2011 2,2′-Bipyridine-6,6′-diyl bisnitroxide as a paramagnetic host: Encapsulation of a zinc(II) ion *Polyhedron* **30** 3034–7
[52] Okazawa A 2017 Magneto-Structural Relationship on Strong Exchange Interactions between Chelating Nitroxide Radical and Transition-Metal Spins *IOP Conference Series: Materials Science and Engineering* **202** 012002
[53] Ishida T, Murakami R, Kanetomo T and Nojiri H 2013 Magnetic study on radical-gadolinium(III) complexes. Relationship between the exchange coupling and coordination structure *Polyhedron* **66** 183–7
[54] Kanetomo T and Ishida T 2014 Strongest Exchange Coupling in Gadolinium(III) and Nitroxide Coordination Compounds *Inorganic Chemistry* **53** 10794–6

[55] Kanetomo T, Yoshitake T and Ishida T 2016 Strongest Ferromagnetic Coupling in Designed Gadolinium(III)–Nitroxide Coordination Compounds *Inorganic Chemistry* **55** 8140–6
[56] Kanetomo T, Kihara T, Miyake A, Matsuo A, Tokunaga M, Kindo K, Nojiri H and Ishida T 2017 Giant Exchange Coupling Evidenced with a Magnetization Jump at 52 T for a Gadolinium-Nitroxide Chelate *Inorganic Chemistry* **56** 3310–4
[57] Homma Y and Ishida T 2018 A New $S = 0 \rightleftarrows S = 2$ "Spin-Crossover" Scenario Found in a Nickel(II) Bis(nitroxide) System *Chemistry of Materials* **30** 1835–8
[58] Kyoden Y, Homma Y and Ishida T 2018 *to be submitted*
[59] Okazawa A and Ishida T 2010 Spin-Transition-Like Behavior on One Side in a Nitroxide-Copper(II)-Nitroxide Triad System *Inorganic Chemistry* **49** 10144–7
[60] Okazawa A, Hashizume D and Ishida T 2010 Ferro- and Antiferromagnetic Coupling Switch Accompanied by Twist Deformation around the Copper(II) and Nitroxide Coordination Bond *Journal of the American Chemical Society* **132** 11516–24
[61] Ovcharenko V, Fokin S, Chubakova E, Romanenko G, Bogomyakov A, Dobrokhotova Z, Lukzen N, Morozov V, Petrova M, Petrova M, Zueva E, Rozentsveig I, Rudyakova E, Levkovskaya G and Sagdeev R 2016 A Copper–Nitroxide Adduct Exhibiting Separate Single Crystal-to-Single Crystal Polymerization–Depolymerization and Spin Crossover Transitions *Inorganic Chemistry* **55** 5853–61
[62] Fedin M V, Veber S L, Bagryanskaya E G and Ovcharenko V I 2015 Electron paramagnetic resonance of switchable copper-nitroxide-based molecular magnets: An indispensable tool for intriguing systems *Coordination Chemistry Reviews* **289–290** 341–56
[63] Gass I A, Tewary S, Rajaraman G, Asadi M, Lupton D W, Moubaraki B, Chastanet G, Létard J-F and Murray K S 2014 Solvate-Dependent Spin Crossover and Exchange in Cobalt(II) Oxazolidine Nitroxide Chelates *Inorganic Chemistry* **53** 5055–66
[64] Sutter J-P, Fettouhi M, Li L, Michaut C, Ouahab L and Kahn O 1996 Synergy between Magnetic Interaction and Spin Crossover in an Iron(III) Complex with an Organic Radical as Ligand *Angewandte Chemie International Edition in English* **35** 2113–6
[65] Ondo A and Ishida T 2018 Cobalt(II) Terpyridin-4′-yl Nitroxide Complex as an Exchange-Coupled Spin-Crossover Material *Crystals* **8** 155
[66] Galyametdinov Y, Ksenofontov V, Prosvirin A, Ovchinnikov I, Ivanova G, Gütlich P and Haase W 2001 First Example of Coexistence of Thermal Spin Transition and Liquid-Crystal Properties *Angewandte Chemie International Edition* **40** 4269–71
[67] Hayami S, Komatsu Y, Shimizu T, Kamihata H and Lee Y H 2011 Spin-crossover in cobalt(II) compounds containing terpyridine and its derivatives *Coordination Chemistry Reviews* **255** 1981–90
[68] Zhang W, Zhao F, Liu T, Yuan M, Wang Z-M and Gao S 2007 Spin Crossover in a Series of Iron(II) Complexes of 2-(2-Alkyl-2H-tetrazol-5-yl)-1,10-phenanthroline: Effects of Alkyl Side Chain, Solvent, and Anion *Inorganic Chemistry* **46** 2541–55
[69] Schlamp S, Weber B, Naik A D and Garcia Y 2011 Cooperative spin transition in a lipid layer like system *Chemical Communications* **47** 7152
[70] Oso Y, Kanatsuki D, Saito S, Nogami T and Ishida T 2008 Spin-crossover Transition Coupled with Another Solid–Solid Phase Transition for Iron(II) Thiocyanate Complexes Chelated with Alkylated N-(Di-2-pyridylmethylene)anilines *Chemistry Letters* **37** 760–1
[71] Oso Y and Ishida T 2009 Spin-crossover Transition in a Mesophase Iron(II) Thiocyanate Complex Chelated with 4-Hexadecyl-N-(2-pyridylmethylene)aniline *Chemistry Letters* **38** 604–5
[72] Ortega-Villar N, Muñoz M and Real J 2016 Symmetry Breaking in Iron(II) Spin-Crossover Molecular Crystals *Magnetochemistry* **2** 16
[73] Kashiro A, Some K, Kobayashi Y and Ishida T 2018 Iron(II) and 1,1,1-Tris(2-pyridyl)nonadecane Complex Showing Order-Disorder Type Structural Transition and Spin-Crossover Synchronized over Both Conformers *to be submitted*

[74] Ishida T, Kanetomo T and Yamasaki M 2016 An iron(II) complex tripodally chelated with 1,1,1-tris(pyridin-2-yl)ethane showing room-temperature spin-crossover behaviour *Acta Crystallographica Section C Structural Chemistry* **72** 797–801
[75] Yamasaki M and Ishida T 2015 Spin-crossover thermal hysteresis and light-induced effect on iron(II) complexes with tripodal tris(2-pyridyl)methanol *Polyhedron* **85** 795–9
[76] Yamasaki M and Ishida T 2015 Heating-rate dependence of spin-crossover hysteresis observed in an iron(II) complex having tris(2-pyridyl)methanol *Journal of Materials Chemistry C* **3** 7784–7
[77] Hirosawa N, Oso Y and Ishida T 2012 Spin Crossover and Light-induced Excited Spin-state Trapping Observed for an Iron(II) Complex Chelated with Tripodal Tetrakis(2-pyridyl)methane *Chemistry Letters* **41** 716–8
[78] Yamasaki M and Ishida T 2015 First Iron(II) Spin-crossover Complex with an N_5S Coordination Sphere *Chemistry Letters* **44** 920–1
[79] Nebbali K, Mekuimemba C D, Charles C, Yefsah S, Chastanet G, Mota A J, Colacio E and Triki S 2018 One-Dimensional Thiocyanato-Bridged Fe(II) Spin Crossover Cooperative Polymer With Unusual FeN_5S Coordination Sphere *Inorganic Chemistry* **57** 12338–46
[80] Létard J-F, Guionneau P, Codjovi E, Lavastre O, Bravic G, Chasseau D and Kahn O 1997 Wide Thermal Hysteresis for the Mononuclear Spin-Crossover Compound *cis*-Bis(thiocyanato)bis[*N*-(2'-pyridylmethylene)-4-(phenylethynyl)anilino]iron(II) *Journal of the American Chemical Society* **119** 10861–2
[81] Bréfuel N, Imatomi S, Torigoe H, Hagiwara H, Shova S, Meunier J-F, Bonhommeau S, Tuchagues J-P and Matsumoto N 2006 Structural−Electronic Correlation in the First-Order Phase Transition of $[FeH_2L^{2\text{-Me}}](ClO_4)_2$ ($H_2L^{2\text{-Me}}$ = Bis[(2-methylimidazol-4-yl)methylidene)-3-aminopropyl]ethylenediamine) *Inorganic Chemistry* **45** 8126–35
[82] Hang H, Fei B, Chen X Q, Tong M L, Ksenofontov V, Gural'skiy I A and Bao X 2018 Multiple spin phases in a switchable Fe(II) complex: polymorphism and symmetry breaking effects *Journal of Materials Chemistry C* **6** 3352–61
[83] Phonsri W, Davies C G, Jameson G N L, Moubaraki B, Ward J S, Kruger P E, Chastanet G and Murray K S 2017 Symmetry breaking above room temperature in an Fe(II) spin crossover complex with an N_4O_2 donor set *Chemical Communications* **53** 1374–7
[84] Mochida N, Kimura A and Ishida T 2015 Spin-Crossover Hysteresis of $[Fe^{II}(L_H^{iPr})_2(NCS)_2]$ (L_H^{iPr} = N-2-Pyridylmethylene-4-Isopropylaniline) Accompanied by Isopropyl Conformation Isomerism *Magnetochemistry* **1** 17–27

Acknowledgments
The author is deeply grateful to the collaborators whose names are listed as co-authors in the references published from author's laboratory, especially to Mr. Kashiro A, Mr. Kyoden Y, Dr. Kanetomo T and Dr. Okazawa A for the recent work. Funding from JSPS KAKENHI (Grant Number 15H03793) is acknowledged.